

Reliable Automatic Calibration of Omni-Cams with Multi-Hypothesis Extended Kalman Filters

Max Fischer

Beuth Hochschule für Technik Berlin, Germany

Thimo Langbehn and Volker Sommer

Beuth Hochschule für Technik Berlin, Germany

Email: {langbehn, sommer}@beuth-hochschule.de

Abstract—This paper presents a method to estimate the two-dimensional mount parameters (offset and rotation) of a bearing only sensor on a mobile robot. It is a continuation of the work done by D. Scaramuzza on auto-calibration of omnidirectional cameras for mobile robots. The system model of the robot is split into two subsystems with reduced complexity, which makes it possible to detect incorrect estimates, as well as to reduce the parameter search space to one dimension for each subsystem. Multiple hypothesis extended kalman-filters (MHEKF) are used to cover a part of the search dimension and the parameter space for a validation parameter. Based on this approach, incorrect estimates can be detected automatically which is a requirement to use calibration methods in a fully automated setting.

Index Terms—omnidirectional camera, calibration, kalman-filter

I. INTRODUCTION

To use or fuse information from a sensor of a mobile robot, a control system has to know how measured signals relate to the environment, and where the sensor is positioned relative to the robot.

In the case of a bearing only sensor (like an omnidirectional camera), its position and orientation relative to the robot kinematic center has to be known. This paper presents an approach to calibrate this relation in a two-dimensional system without human interaction. In the existing literature, the term (omnidirectional) camera calibration is mostly used to describe the extraction of optical parameters (e.g. focal length, mirror curvature etc.) used in the mapping between the environment and the camera sensor chip, and therefore the resulting image ([1],[2],[3]). In this paper, those optical parameters are assumed to be correct, and the parameters to be calibrated refer to the spatial relation of the camera sensor with respect to the mobile robot base. Since the investigated system has two dimensions, the optical axis of the camera sensor is assumed to be orthogonal to the movement plain. A method to calibrate an existing offset angle for this axis is described in [4].

The examples are based on vertical edge detection in images from an omnidirectional camera, but the presented method works with any kind of bearing only sensor, assuming it provides identification information, for example by feature tracking ([5]) or feature identification algorithms.

If fully automatic systems are used to calibrate essential parameters for mobile robots, it will be important that they are able to handle all situations, or at least to identify those situations which prevent them from working correctly. In this paper, the approach presented in [6] and [7] is modified to make the calibration more robust and to improve the success rate by reducing the available trajectories.

The base system presented in section II is based on the model described in [6]. The system observability highly depends on the robot trajectory. Since the trajectories required to observe the states are already known from [6], the system is split into two smaller systems limited exclusively to either straight motion or pure rotation (section III) which are then used in Extended Kalman-Filters (see [8]) to estimate the system states. The circumstances in which the subsystems are not locally observable (see [9] and [10]) are analyzed, too.

Section IV describes the criteria by which the correctness of an estimate can be deduced as well as the influence of the initial state values and section V presents a procedure to acquire correct estimates.

II. SYSTEM STATE MODEL

The two dimensional model used to describe the relation between the robot, its camera and the measured feature shown in Fig. 1 is similar to that introduced by [6] and leads to the state model given in (1).

$$\chi_{i+1} = \begin{bmatrix} D_{i+1} = D_i + \delta s_i \cos(\theta_i) \\ \theta_{i+1} = \theta_i + \delta\theta_i - \frac{\delta s_i}{D_i} \sin(\theta_i) \\ \phi_{i+1} = \phi \\ \rho_{i+1} = \rho \\ \psi_{i+1} = \psi \end{bmatrix} \quad (1)$$

Manuscript received September 15, 2013; revised December 4, 2013.

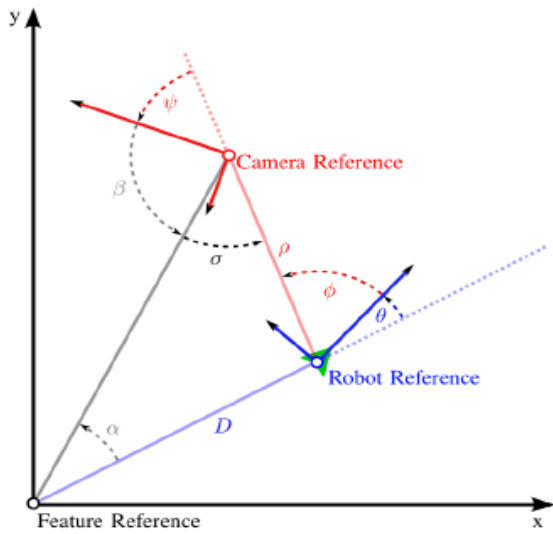


Figure 1. System reference in environment.

The system state consists of five parameters; φ , ρ and ψ describe the (two dimensional) camera pose in relation to the robot kinematic center, while D and θ describe the robot pose in relation to an observed feature. The orientation of the feature is not required since it does not influence the measured bearing signal β .

The input signals of the system are the incrementally traveled distance (straight forward) of the robot δs and the small difference in robot orientation relative to the feature reference system $\delta\theta$, which form the input vector $u = [\delta s, \delta\theta]$. Since the model is based on a bearing only sensor, the measurement contains only the feature angle β (camera relative).

Note that the description of the system dynamics in (1) is approximated and applies only to small δs .

The calibration aim is to find accurate values for the camera pose parameters φ , ρ and ψ using only the odometry input (δs and $\delta\theta$) and the measured feature angle β .

According to figure 1 the expected angle β with respect to the state x follows as (2).

$$\begin{aligned} \alpha &= \text{atan2}(\rho \sin(\theta + \varphi), D + \rho \cos(\theta + \varphi)) \\ \sigma &= \varphi + \theta - \alpha \\ \beta &= \pi - \psi - \sigma \end{aligned} \quad (2)$$

A. Observability Analysis

The observability of the given system is investigated using the method proposed by [10]. Gradients of the dynamics are derived by using the Lie-Derivation in each direction of the input signals, and are subsequently combined into the observability matrix $Q(x)$. The system is observable if the determinant $\det(Q(x))$ of this matrix is not zero. Note that, in contrast to linear systems, the observability of non-linear systems in general depends on its current state and input signals.

For this system, the determinant as derived in the appendix is

$$\det(Q) = \frac{abc}{(D^2 + \rho^2 + 2D\rho \cos(\theta + \varphi))^{10}}$$

with

$$\begin{aligned} a &= 4D^3 \rho^2 \sin(\theta + \varphi)^2 (0.5D^2 - 0.5\rho^2) \\ b &= 2D\rho \sin(\varphi) - D^2 \sin(\theta) + \rho^2 \sin(2\varphi + \theta) - \rho^3 \sin(2\varphi + \theta) \\ c &= 2D^3 \rho \cos(\theta + \varphi) - D^4 + 6D^2 \rho^2 + 2D\rho^3 \cos(\theta + \varphi) - \rho^4 \end{aligned}$$

The determinant of this system depends on its state x , which in turn depends on the initial state x_0 and the system input. In other words, the observability of the system depends on the robot trajectory with respect to the measured feature.

The determinant trace $\det(Q(x))$ for a circle trajectory with the landmark outside of the circle contains several states at which the system is not observable, for example if the angle θ is near $k\pi$ with $k \in \mathbb{N}$, which is caused by the robot driving towards or away from the feature. In this case there are no changes in the measure signal β and therefore the system becomes not observable. The same happens if the signal variations β becomes weak due to a large distance between the feature and the robot, because of

$$\lim_{D \rightarrow \infty} \det(Q) = 0$$

III. OBSERVABLE SUBSYSTEMS

Since for example a circle trajectory contains several not observable states it is hard to construct a reliable EKF on the basis of this full system state model. However, by reducing the dimension of the input vector, the conditions for the observability of the resulting subsystems get much simpler.

The state observability depends on the distance of the omniscam sensor relative to the feature distance, therefore

the case $\frac{D}{\rho} \gg 1$ is excluded (see [7] for an analysis) and the system is split into subsystems considering exclusively straight motion and pure rotation.

A. Subsystem for Straight Motion

In this case the robot system is only driving on a straight line ($\delta\theta = 0$). If the robot is driving a distance of δs , the camera will move forward the same distance, as well (see figure 2, C is the distance between feature and camera). This system is based on the approximately equal position of the camera and robot ($C \approx D$ and $\zeta \approx \theta$), therefore it is only valid for a feature that is sufficiently far away in

relation to the camera offset ρ $\frac{D}{\rho} \gg 1$. The system model is given in (4) and the corresponding measurement model in (5). For this system, the camera offset ρ in relation to the robot is not observable, changing it will not alter the input

signal as long as the tracked landmark remains at the same camera-relative position¹.

$$\eta := \psi + \phi \quad (3)$$

$$\underline{x}_{i+1} = \begin{bmatrix} C_{i+1} = C_i + \delta s_i \cos(\zeta_i) \\ \zeta_{i+1} = \zeta_i - \frac{\delta s_i}{\zeta_i} \sin(\zeta_i) \\ \eta_{i+1} = \eta_i \end{bmatrix} \quad (4)$$

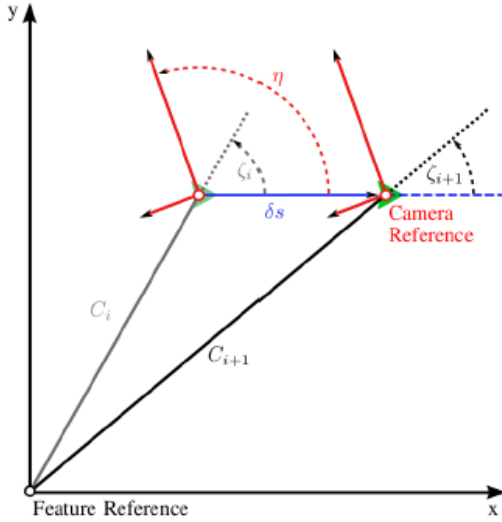


Figure 2. Translation only subsystem.

The observability analysis of this system leads to (6). This subsystem is observable only if $\theta c = k\pi$ with $k \in \mathbb{N}$. In other words, if the camera is moving to or from the feature then the states of this subsystem are not observable. Further, since

$$\det(\underline{Q}) = 2 \frac{\sin(\zeta)}{C^4} \quad (6)$$

$$\lim_{C \rightarrow \infty} \det(\underline{Q}) = 0$$

the observability degrades if the feature is far away.

B. Subsystem For Pure Rotation

In this case the robot system only rotates about its own center. The system model is reduced to (9), and the measurement model to (10) (see Fig. 3 for the used variables).

$$\lambda := \frac{D}{\rho} \quad (7)$$

¹This is easily verified if one thinks of it as moving the robot while the Camera remains fixed. As long as the robot orientation remains unchanged,

The δs of the robot will always result in the same movement for the camera.

$$\gamma := \theta + \phi \quad (8)$$

$$\underline{x}_{i+1} = \begin{bmatrix} \lambda_{i+1} = \lambda \\ \gamma_{i+1} = \gamma_i + \delta\theta \\ \psi_{i+1} = \psi_i \end{bmatrix} \quad (9)$$

$$\beta(\underline{x}) = \pi + \text{atan2}(\sin(\gamma), \lambda + \cos(\gamma)) - \psi - \gamma \quad (10)$$

$$\det(\underline{Q}) = \frac{-\lambda(\lambda^2 - 1)}{(\lambda^2 + 2\lambda\cos(\gamma) + 1)^3} \quad (11)$$

According to the determinant of the observability matrix (11), the system is not observable if $\lambda = 0$, but it can be assumed that the feature is farther away from the robot as the camera sensor ($\lambda > 1$) since they might collide otherwise. However, due to 12 in the case of a huge λ , the system becomes also not observable. This leads to the same conclusion as in [2], that the robot has to be quite close to the feature for the subsystem with pure rotation.

$$\lim_{\lambda \rightarrow \infty} \det(\underline{Q}) = 0 \quad (12)$$

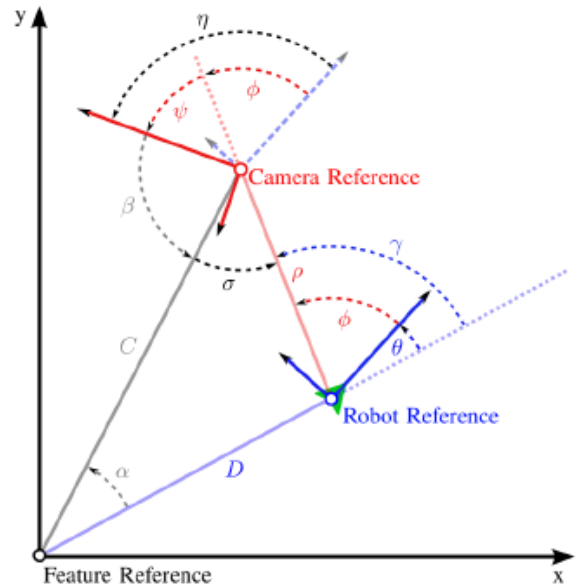


Figure 3. Pure rotation system with support angles.

C. Target State Extraction

By means of using both subsystems it is feasible to extract the target states ϕ , ρ and ψ . The angle ψ is directly provided by the pure rotation subsystem, and ϕ can be calculated using (13).

$$\phi = \eta - \psi \quad (13)$$

(14) and (15) follow from Fig. 3 and with $\lambda = \frac{D}{\rho}$ from (9) this leads to (16) which provides two possible solutions for ρ . This ambiguity can be resolved by measuring an additional feature, since both measurements must yield the same distance ρ .

$$\sigma = \pi - \beta - \psi \quad (14)$$

$$D^2 = D_c^2 + \rho^2 - 2D_c\rho\cos(\sigma) \quad (15)$$

$$\lambda^2 = 1 + \frac{C^2}{\rho^2} - \frac{2C\rho\cos(\sigma)}{\rho}$$

$$\Rightarrow \lambda^2\rho^2 - \rho^2 - C^2 + 2C\rho\cos(\sigma) = 0$$

$$\Rightarrow \lambda^2\rho^2 - \rho^2 - C^2 + 2C\rho\cos(\sigma) = 0$$

$$\Rightarrow \rho_{1,2} = \frac{-C\cos(\sigma)}{\lambda^2 - 1} \pm \sqrt{\left(\frac{C\cos(\sigma)}{\lambda^2 - 1}\right)^2 + \frac{C^2}{\lambda^2 - 1}}$$

$$\rho_{1,2} = \frac{C}{\lambda^2 - 1} \left(-\cos(\sigma) \pm \sqrt{\lambda^2 - 1 + \cos^2(\sigma)} \right) \quad (16)$$

After the target states are known, D and θ for the feature follow as $D = \lambda\rho$ and $\theta = \gamma + \sigma - \varphi$.

IV. SIMULATION RESULTS

A well chosen trajectory that leads to an observable system is a necessary condition to find the correct solution, however it is not sufficient if the calibration trajectory is finite. In this case the correct estimation depends on the initial value for the system state as well. Depending on the trajectory and the initial values, the EKF might converge on a local minimum or not converge at all. To get around this problem, a Multi-Hypothesis EKF is initialized with several samples of the configuration space.

The system behaviour and its parameter dependence was investigated using a simulation environment that contains only one feature in the point of origin. In this example, the robot performs a straight motion of four meters and subsequently rotates five times on the spot. The camera position relative to the robot is set as $\varphi = 1.10\text{rad}$, $\rho = 0.223\text{m}$ and $\psi = 1.68\text{rad}$. The input signal is modified with added Gaussian noise (standard deviation of two percent) to simulate wheel slip. The resolution of the measurement signal is one degree and Gaussian noise with one degree standard deviation is added to the signal.

This and other simulation runs were used to investigate per-formance of the estimation system as well as its dependance on the initial state values.

A. Straight Motion

Based on (6), the observability of the straight motion subsystem depends on C and ζ , and of course on the measurement signal β . The biggest dynamic range of the measurement signal is provided if the robot drives past (but not through) the feature. In this case the measured signal follows the arc tangent function and the inflection point corresponds to the place where the robot is passing the feature. In addition to the trajectory, the stability and accuracy of the EKF depends on the start values of the state

(C_0, ζ_0, η_0) as well, since wrong start values might lead to incorrect local minima. In fact, the state dimensions influence the filter in varying degrees.

For a poorly² chosen C_0 the filter will not reach a correct estimation (indicated by the innovation not converging to 0) regardless of the used ζ_0 . A good choice of C_0 results in correct estimates regardless off the ζ_0 and η_0 values. In that case, the filter converges quickly after passing the feature (widest dynamic range for β). Fig. 4 and Fig. 5 show the estimation process for different ζ_0 and a common, good C_0 . Each case results in the correct ζ value with the innovation converging to zero.

This example and many other simulation results indicate that of all initial values, only C_0 is critical with regard to a correct result. The angle η is not even contained in the observability criterion (6). An indicator for the correctness of an estimate is provided by the EKF innovation combined with the ζ value. For a good estimate, the innovation of the EKF should converge to zero and ζ should converge to the same value for all ζ_0 .

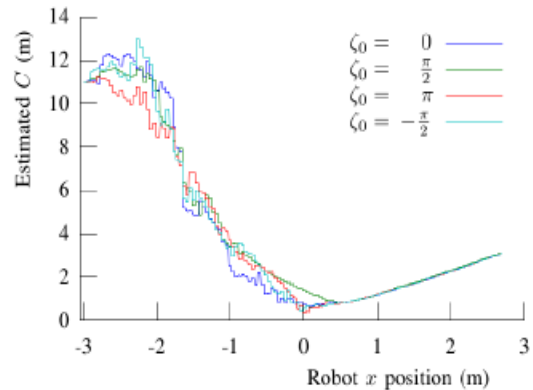


Figure 4. Straight movement $-C$ for a good C_0

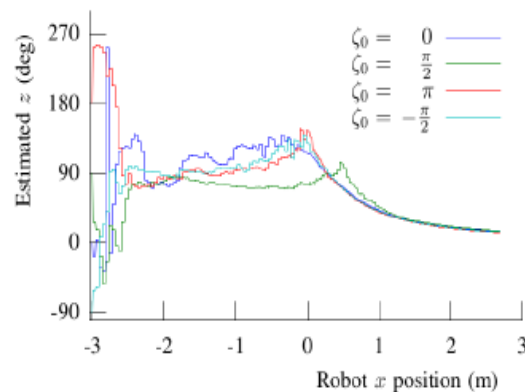


Figure 5. Straight movement $-\zeta$ for a good C_0

²The word poorly here does not refer to the deviation of a parameter from its correct value. Instead, it just means the effect of a chosen starting Value on convergency of the EKF.

B. Pure Rotation

In contrast to the case with straight motion it is difficult to use the measurement signal in order to detect the observability of the rotation system states. To solve this problem, several filters with different starting values are used again. If they converge to different values then the system is not observable based on the given measurement data. For each of the following cases, the robot rotates five times, and the collected measurement data is fed into the EKFs with their different start values.

In the first case the robot trajectory is set so far away from the feature that the system states became not observable. For several filters with varying γ_0 , each EKF estimates different values of the state γ while the innovation converges to zero. This ambiguity in the result indicates that the system states are not observable.

In the second case the trajectory leads to observable system states, but the λ_0 value was too small. The course of the γ state estimation is similar to the previous case, however in this case the innovation does not converge to zero but oscillates with the frequency of the robot rotation.

In the third case, λ_0 was set to a common, benign value and the γ_0 and ψ_0 values were varied. Each of the EKFs estimate the correct γ value and the innovation of each EKF converges to zero (See figure 6 and 7).

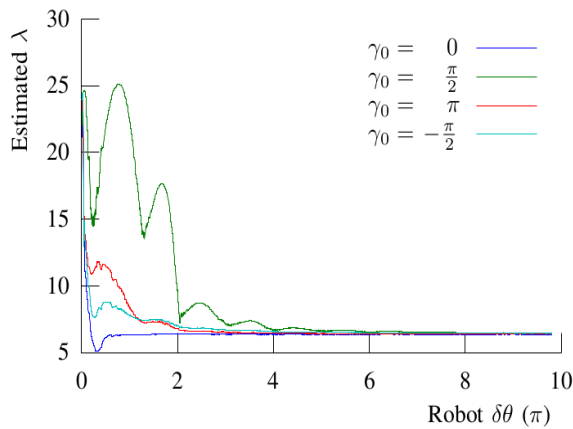


Figure 6. Rotation - λ for a good λ_0

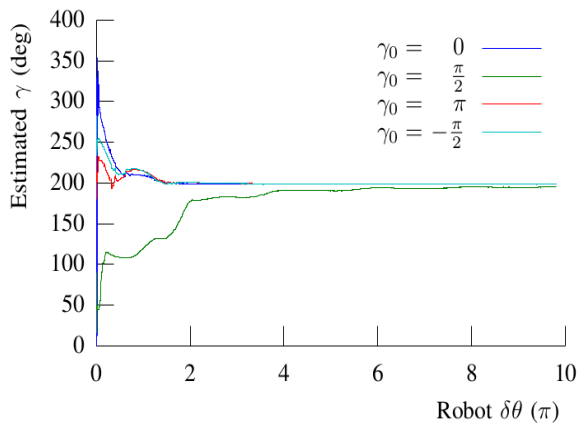


Figure 7. Rotation - γ for a good λ_0

This example and various simulations indicate that the values for γ_0 and λ_0 are negligible, but λ_0 has a critical impact on the correct result. Again, multiple filters can be used to cover the value range of λ_0 . However, to detect unobservable situations caused by a large feature distance, multiple γ_0 have to be used for each λ_0 as well.

C. Target State Calculation

With the results above, the target states can be calculated as $\varphi = 1.12$, $\psi = 1.675$, $\rho_1 = 0.219\text{m}$ and $\rho_2 = -0.258\text{m}$. The ambiguity between ρ_1 and ρ_2 can be resolved by observing a second feature. As shown above, the estimations are robust, although their accuracy is limited by the signal noise and available measurement resolution.

V. ROBUST PARAMETER ESTIMATION

As explained above, it is possible to estimate the pose parameters for an omnidirectional camera using a simple calibration sequence given that detectable features are close enough. To remove ambiguities and incorrect estimates, it is necessary to track multiple features and to eliminate those that are not observable.

To make the calibration process efficient, the following sequence is recommended:

A. Straight Motion

- 1) Perform a straight motion and log the robot trajectory as well as the sensor data (bearing) of visible features.
- 2) Discard all features which were not passed by the robot. The robot passed a feature if its bearing angle follows an arcus tangens function.
- 3) Use an EKF to estimate the states C , ζ and η of each feature. Eliminate errors caused by incorrect C_0 values by using multiple estimation with different C_0 values.
- 4) If no correct solution was found, expand the range of the used C_0 and go back to (c). Simulations indicate that benign C_0 exist in the range $(0, 4D_{\max}]$ with D_{\max} being the maximal real distance of the landmark.

B. Pure Rotation

- 1) Perform several (five) pure rotations and log the robot trajectory as well as the sensor data of all visible features.
- 2) Create a set of EKFs with different λ_0 values for each feature.
- 3) Select the best λ_0 value for each feature of those that do not result in oscillating innovation.
- 4) Create a set of EKFs with different γ_0 values for each feature (using the previously selected λ_0).

5) Eliminate all features whose Filters do not converge to a common γ .

C. Calculate the Camera Pose Parameters and Resolve the ρ Ambiguity by Comparing the Results of Several Features.

VI. CONCLUSION

While the resulting systems do depend on a somewhat Combining them and substituting fixed trajectory pattern, they provide estimates which can be automatically rated with regard to their correctness. Since estimation errors due to bad start values can be detected and avoided, the results depend only on the distance and the straight motion path. If multiple features are available, the favourable ones will lead to correct estimates faster. In combination, this can be used to move the robot on a favourable trajectory to reduce the time required to get a good estimate.

APPENDIX

As shown in [1], the observation analysis is performed by using Lie derivatives. With the input direction vectors

$$f_1 = \left[\cos(\theta), -\sin\left(\frac{\theta}{D}\right), 0, 0, 0 \right]^T$$

$$f_2 = [0, 1, 0, 0, 0]^T$$

the Lie derivatives follow

$$L^0 \beta = \beta$$

$$L_{f_1}^1 \beta = \frac{D \sin(\theta) - \rho \sin(\phi)}{\gamma}$$

$$L_{f_2}^1 \beta = \frac{-D^2 - D\rho \cos(\phi + \theta)}{\gamma}$$

$$L_{f_1, f_2}^2 \beta = \frac{D(\rho^2 \cos(2\phi + \theta) + D^2 \cos(\theta) + 2D\rho \cos(\phi))}{\gamma^2}$$

$$L_{f_2, f_2}^2 \beta = \frac{D\rho \sin(\phi + \theta)(D^2 - \rho^2)}{\gamma^2}$$

Combining them and substituting

$$\gamma = D^2 + \rho^2 + 2D\rho \cos(\phi + \theta)$$

leads to the observation matrix

$$Q(x) = \begin{bmatrix} \frac{\partial L^0}{\partial x_1} & \cdots & \frac{\partial L^0}{\partial x_5} \\ \vdots & \cdots & \vdots \\ \frac{\partial L_{f_2, f_2}^2}{\partial x_1} & \cdots & \frac{\partial L_{f_2, f_2}^2}{\partial x_5} \end{bmatrix}$$

and its determinant of

$$\det(Q) = \frac{abc}{(D^2 + \rho^2 + 2D\rho \cos(\theta + \phi))^{10}}$$

with

$$a = 4D^3 \rho^2 \sin(\theta + \phi)^2 (0.5D^2 - 0.5\rho^2)$$

$$b = 2D\rho \sin(\phi) - D^2 \sin(\theta) + \rho^2 \sin(2\phi + \theta) - \rho^3 \sin(2\phi + \theta)$$

$$c = 2D^3 \rho \cos(\theta + \phi) - D^4 + 6D^2 \rho^2 + 2D\rho^3 \cos(\theta + \phi) - \rho^4$$

REFERENCES

- [1] J. Fabrizio, J. P. Tarel, and R. Benosman, "Calibration of panorami catadioptric sensors made easier," in *Proc. Third Work-shop on Omnidirectional Vision*, 2002.
- [2] N. D. Jankovic and M. D. Naish, "Calibrating an active omni-directional vision system," in *Proc. International Conference on Intelligent Robots and Systems*, August 2005, pp. 3093–3098.
- [3] L. Puig, J. Bermúdez, P. F. Sturm, and J. J. Guerrero, "Calibration of omnidirectional cameras in practice: A comparison of methods," *Computer Vision and Image Understanding*, vol. 116, no. 1, pp. 120–137, 2012.
- [4] L. Puig, J. Bermudez, and J. Guerrero, "Self-orientation of a hand held catadioptric system in man-made environments," in *Proc. IEEE International Conference on Robotics and Automation*, Anchorage, AK, May 2010, pp. 2549–2555.
- [5] T. Tasaki, S. Tokura, T. Sonoura, F. Ozaki, and N. Matsuhira, "Mobile robot self-localization based on tracked scale and rotation invariant feature points by using an omnidirectional camera," in *Proc. IEEE/RSJ International Conference on Intelligent Robots and Systems*, 2010.
- [6] D. Scaramuzza, "Omnidirectional vision: From calibration to robot motion estimation," PhD thesis, ETH Zurich, 2008.
- [7] D. Scaramuzza, A. Martinelli, and R. Siegwart, "A robust descriptor for tracking vertical lines in omnidirectional images and its use in mobile robotics," *International Journal of Robotics Research*, vol. 28, pp. 149–171, February 2009.
- [8] R. E. Kalman, "A new approach to linear filtering and prediction problems," *Journal of Basic Engineering*, Modern transcription of the original article by John Lukesh January 2002, vol. 82, pp. 35–45, 1960.
- [9] R. Hermann and A. J. Krener, "Nonlinear controllability and observability," *IEEE Transactions on Automatic Control*, vol. 22, pp. 728–740, October 1977.
- [10] J. Adamy, *Nichtlineare Regelungen*, Springer, 2009.